

Analysis and applications of beam propagation method and coupled-mode theory

A. SELVARAJAN AND R. BALASUBRAMANIAN

Department of Electrical Communication Engineering, Indian Institute of Science, Bangalore 560 012, India.

Received on February 6, 1995. Revised on March 19, 1996

Abstract

Understanding of light propagation in fiber and integrated optical waveguides is important in designing efficient guided wave optical structures. Depending on the complexity of the devices, various analytical and numerical methods of analysis have been developed by many groups. Two of the popular methods are beam propagation method (BPM) and coupled-mode theory. Our group has, with certain modifications and improvements, applied these theories to study a few integrated optic (IO) devices. These include light propagation in planar and channel waveguide bends, coupling of light from fiber to IO waveguide and Cerenkov second harmonic generation. Theoretical derivations and some results are reviewed in this paper.

Keywords: Beam propagation method (BPM), coupled-mode theory (CMT), integrated optic devices, optical fibers, semiconductor lasers, photonics.

1. Introduction

The advent of optical fibers and semiconductor lasers was largely responsible for the rapid and revolutionary changes in the whole gamut of communication, computing, sensing and signal processing using photonics. A basic building block in photonics is the optical waveguide which traps and transports light waves in the form of well-defined modes. Two types of optical waveguides are important. The cylindrical-type single and multimode fibers of silica glass are the most appropriate for long-distance transmission and also certain sensing and signal-processing applications. Planar and channel waveguides are the workhorse in integrated optics and optical ICs. The field of optical communication has assumed tremendous importance in terms of high information-carrying capacity. Integrated optics (IO) is expected to play an increasing role in optical signal processing at the transmitting and receiving ends and at the point of regeneration. Here one builds various functional devices and circuits like power splitter, modulator, multiplexer, amplifier, switch, etc., using thin-film technologies. The study of light propagation through waveguide structures is an important area as it enables the design and fabrication of well-defined single-mode waveguides and devices with precise performance characteristics. Over the years the theory of dielectric optical waveguides has become well established. The range of methods varies from direct methods when the waveguides are simple (*e.g.*, planar step index waveguides) to coupled-mode theory and other approaches which are required to tackle complex waveguides. Our group has been active for over five years in the field of analysis and design of waveguides and

waveguide devices. Two of the most commonly used methods in this context are the beam propagation method (BPM) and coupled-mode theory (CMT). An outline of the basic theory and some applications of BPM and CMT are presented in this review.

2. Beam propagation method (BPM)

2.1. Fourier transform (FT) BPM

BPM is a transform technique where, given an input beam $\psi(x)$ at $z = 0$ along the propagation direction, the output beam at $z = L$ is obtained in two steps. In the first step the field, $\psi(x, L)$, that would have propagated in a homogeneous structure $n_0^2(x)$ is obtained. This is easily done, for example, by multiplying the Fourier components of the input beam by the corresponding phase factor $\exp(-j\beta z)$. In the second step, the resulting propagated field is multiplied by a correction factor, $\exp(-j\Gamma)$. This is repeated in a number of steps. We now present the essential formulas of BPM^{1,2} (for one propagation step $z = 0$ to Δz).

The propagation of light in a medium can be described by a scalar wave equation

$$\nabla^2 \psi + k_0^2 n^2(x, z) \psi = 0 \quad (1)$$

where $k_0 = \omega/c$, ω , the angular frequency of light, and ∇^2 , the Laplacian operator. Next, the refractive index $n(x, z)$ is split into two parts and is written as

$$n(x, z) = n_s(x, z) + \Delta n(x, z) \quad (2)$$

where $n_s(x, z)$ is the refractive index of the homogeneous (unperturbed) medium and is assumed to be constant. $\Delta n(x, z)$ is taken to be a small perturbation compared to $n_s(x, z)$. The solutions of the wave equation for the unperturbed medium can be readily obtained by solving the wave equation

$$\nabla^2 \phi + k_0^2 n_s^2(x, z) \phi = 0. \quad (3)$$

The required field $\psi(x, z = \Delta z)$ can be written as a product of the field $\xi(x, z = \Delta z)$ propagated in the unperturbed medium and a correction factor Γ as below

$$\psi(x, z = \Delta z) = \xi(x, z = \Delta z) \exp(-j\Gamma) \quad (4)$$

where ξ satisfies the Helmholtz equation

$$\nabla^2 \xi + k_0^2 n_s^2(x, z) \xi = 0. \quad (5)$$

Here it is assumed that $\psi(x, 0) = \xi(x, 0)$. Also $\xi(x, \Delta z)$ can be expressed as

$$\xi(x, \Delta z) = \sum_{m=1}^{\infty} A_m \phi_m(x) \exp(-j\beta_m \Delta z) \quad (6)$$

$$A_m = \int_{-\infty}^{\infty} \xi(x, 0) \phi_m^*(x) dx. \quad (7)$$

The correction factor Γ has been obtained using the paraxial approximation in the scalar wave equation as²,

$$\Gamma = k_0^2 \frac{\Delta n^2(x, z)}{2\beta_x} \Delta z \approx k_0 \Delta n \Delta z. \quad (8)$$

Here $\xi(x, \Delta z)$ is the beam propagated in unperturbed medium $n_r(x, z)$, $\Delta n^2(x, z) = (n^2 - n_r^2)$ and $\beta_x = 2\pi/\lambda n_x$, the propagation constant in the unperturbed medium. The computations are done for a point in the interval $(0, \Delta z)$. Propagation in homogeneous medium can be computed by replacing eqns (6) and (7) by an equivalent FT pair as below:

$$\xi(x, \Delta z) = \frac{1}{2\pi} \int_{-\infty}^{\infty} \tilde{\xi}(k_x, \Delta z) \exp(jk_x x) dk_x, \quad (9)$$

$$\tilde{\xi}(k_x, 0) = \int_{-\infty}^{\infty} \xi(x, 0) \exp(-jk_x x) dx \quad (10)$$

$$\tilde{\xi}(k_x, \Delta z) = \tilde{\xi}(k_x, 0) \exp(-j\beta \Delta z) \quad (11)$$

where

$$\beta = (k_0^2 n_r^2 - k_x^2)^{1/2}. \quad (12)$$

To solve the above equations, Simpson's 1/3 rule can be used. But it would need $2N + 1$ complex multiplications and additions for each value of k_x , where $2N$ is the number of samples taken for integration. If $\tilde{\xi}(k_x)$ is calculated $2N$ times, then $2N(2N + 1)$ complex multiplications and additions will be needed. To reduce the number of complex multiplications, we have used Simpson's 1/3 rule combined with fast Fourier transform (FFT) so that the total number of complex multiplications reduce to $4N \log N$. Also the speed of FFT and accuracy of Simpson's 1/3 rule is simultaneously achieved. We have applied the above theory to bent waveguides, y-branches, directional couplers and X-switches in IO form³. As an example, to find the field in integrated optic structures we have used the modified BPM to study a bent waveguide. Figure 1 shows a typical field variation as a function of propagation distance. The power in the waveguide region can then be calculated using the field obtained. It is found that when the bent angle is large, most of the power is radiated out of the waveguide. For example, when a Gaussian input beam with a refractive index $n_r = 2.1398$ and $\Delta n = 0.1$ is used, and the output power after a propagation distance of $150 \mu\text{m}$ with a bent angle of 3° is calculated, then nearly 70% of the power is found to be within the waveguide. If we increase the bent angle, to about 10° , only 10% of the power remains within the guide. Thus BPM enables a proper design of integrated optic structures taking into account the possible losses at bends in waveguides.

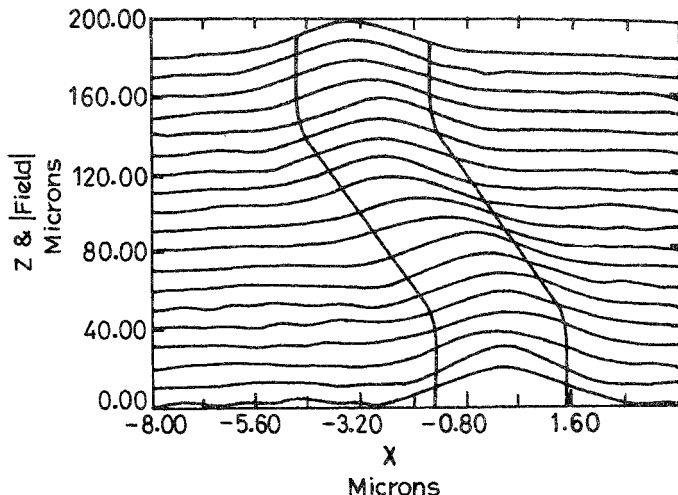


FIG. 1. Field in a bent waveguide using BPM with Gaussian input beam, $n_1 = 2.1398$ and $\Delta n = 0.1\%$

It may be mentioned that the BPM described above solves the Helmholtz equation directly. A limitation of the method is that computations can be carried out only over a limited propagation distance. Also, the refractive index variation must be small to keep the errors within limits. We have developed a transform technique in place of BPM in which such limitations can be overcome. The method converts the partial differential equation into a set of algebraic equations in the transform domain which can be solved on a computer⁴.

2.2. Finite-difference (FD) BPM

As mentioned earlier, the limitations of FT-BPM are that computations can be carried out only over a limited propagation distance and limited computational window, and that the refractive index variation must be small. An alternative approach to FT-BPM could be FD-BPM. We have used this method to study the coupling of light from fiber to IO as discussed below⁵.

The scalar Helmholtz equation can be written in the operator formalism as

$$\frac{\partial \psi}{\partial z} = H \psi \quad (13)$$

where the operator H is given by

$$H = \frac{1}{2jk_0 n_r} \left[\nabla_t^2 + k_0^2 (n^2(x, y, z) - n_r^2) \right] \quad (14)$$

Here n_r is a suitably chosen mean refractive index, k_0 , the wave number in vacuum and ∇_t^2 , the Laplacian in transverse coordinates. Replacing the linear operator H by FD approximation, the paraxial wave equation can be approximated as an explicit difference equation, given by

$$\frac{\partial \psi}{\partial z} = \frac{i}{2jk_0 n_r} \left[a^+ \psi_{p+1,q} + a^- \psi_{p-1,q} + b^+ \psi_{p,q+1} + b^- \psi_{p,q-1} + c \psi_{p,q} \right] \quad (15)$$

where

$$\begin{aligned} a^+ &= \frac{2}{\Delta x_p (\Delta x_p + \Delta x_{p-1})} \\ a^- &= \frac{2}{\Delta x_{p-1} (\Delta x_p + \Delta x_{p-1})} \\ b^+ &= \frac{2}{\Delta y_q (\Delta y_q + \Delta y_{q-1})} \\ b^- &= \frac{2}{\Delta y_{q-1} (\Delta y_q + \Delta y_{q-1})} \\ c &= \left[-a^+ - a^- - b^+ - b^- + k_0^2 (n_{pq}^2 - n_r^2) \right] \end{aligned}$$

As shown in Fig. 2, for every point in the $z + \Delta z$ plane, we need 5 points in the z -plane. Hence this method is called the 5-point difference formula. In the above equation, ψ_{pq} and n_{pq} are the optical field values and the sampled refractive index values, respectively, at $x = x_p$, $y = y_q$ in the computational window and $\Delta x_p = x_p - x_{p-1}$ and $\Delta y_q = y_q - y_{q-1}$.

The above equation is solved numerically for specific cases. Both implicit and explicit FD algorithms were derived which were applied for the analysis of evanescent coupling between fiber and planar waveguides⁵, curved optical waveguides and electrooptic waveguide modulator⁶. Figure 3 shows numerical simulation on the evanescent coupling between the fiber and the planar waveguide. It is seen that there is a periodic exchange of power from fiber to waveguide along the propagation direction. The case shown is for $n_f = n_r$, i.e., planar guide index and fiber index are the same. From such studies an optimum coupling configuration in terms of index profiles, interaction length, etc., can be arrived at.

3. Coupled-mode theory and applications

Many physical systems can be modelled as an interaction between (or among) a number of component systems. Such phenomena are called coupled phenomena and such systems

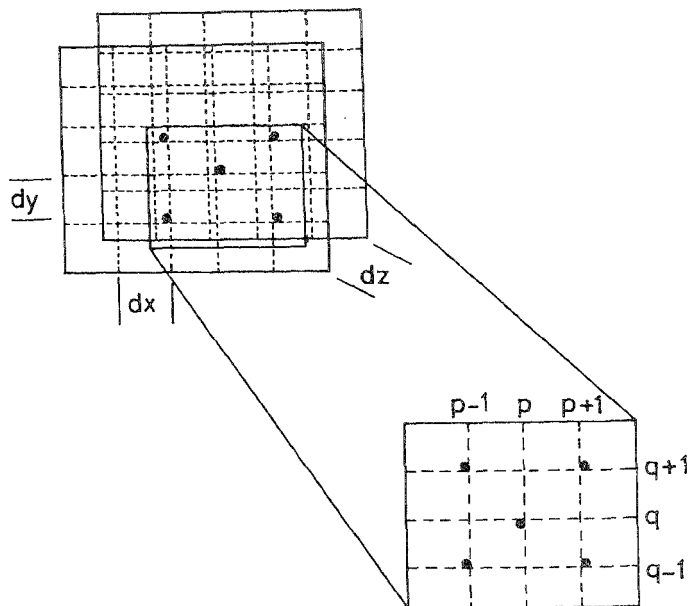


FIG. 2. 5-point finite-difference scheme.

are called coupled systems. The essence of CMT is to determine the coupling coefficients and coupling equations from the properties of component subsystems. For example, the coupled conditions between two optical waveguides when in close proximity can be analysed in terms of the normal modes of the two waveguides when they are far apart. CMT can be applied to solve many problems in the field of fiber and integrated optics, such as analysis of waveguide arrays, periodic, nonparallel, nonlinear and externally perturbed waveguides. Various approaches have been reported for the derivation of the coupled-mode equations⁷. We have considered a derivation of scalar coupled-mode equations as outlined below.

3.1. Coupled-mode equations from scalar wave equation

Consider an N -waveguide system. The eigen mode of such a system can be written as the linear combination of individual interacting modes as follows:

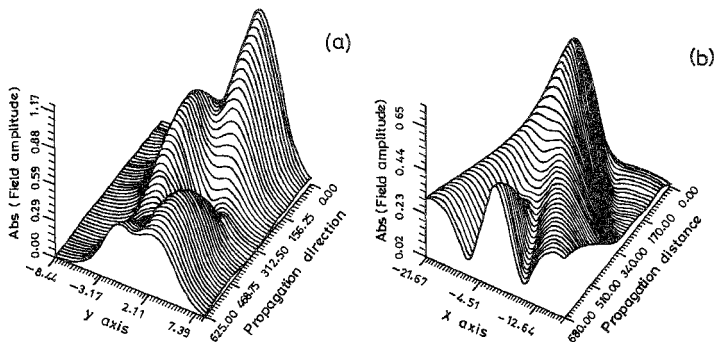


FIG. 3. Evanescent coupling between fiber and planar waveguide. (a) field amplitude in z - y plane, and (b) field amplitude in z - x plane.

$$\Psi(x, y, z) = \sum_{p=1}^N U_p(z) \psi_p(x, y). \quad (16)$$

The functions ψ_p and $U_p(z)$ are the individual mode fields and their weightages. Substituting the eigen-mode expression in the scalar wave equation, we obtain,

$$\sum_{p=1}^N \left\{ U_p \nabla_T^2 \psi_p + \frac{d^2 U_p}{dz^2} \psi_p + k_0^2 n^2 U_p \psi_p \right\} = 0 \quad (17)$$

where ∇_T^2 is the transverse Laplacian. Consider U_p in terms of their envelopes, so that

$$U_p(z) = A_p(z) \exp(-i\beta_p z). \quad (18)$$

When variation of A_p is small compared to $\exp(-i\beta_p z)$ which is true even for strong couplings, second derivative of U_p can be neglected (this is known as the slowly varying approximation). We get,

$$\begin{aligned} \frac{d^2 U_p}{dz^2} &= \left(\frac{d^2 A_p}{dz^2} - 2i\beta_p \frac{dA_p}{dz} - \beta_p^2 A_p \right) \exp(-i\beta_p z) \\ &\approx \left(-2i\beta_p \frac{dA_p}{dz} - \beta_p^2 A_p \right) \exp(-i\beta_p z). \end{aligned} \quad (19)$$

From eqn 18,

$$\frac{dA_p}{dz} = \left(\frac{dU_p}{dz} + i\beta_p U_p \right) \exp(i\beta_p z). \quad (20)$$

Hence,

$$\frac{d^2 U_p}{dz^2} = -2i\beta_p \frac{dU_p}{dz} + \beta_p^2 U_p. \quad (21)$$

Substituting for $d^2 U_p/dz^2$ in eqn 17, we get

$$\sum_p \left\{ (\nabla_T^2 + k_0^2 n^2 - \beta_p^2) \psi_p U_p + \left(2\beta_p^2 U_p - 2i\beta_p \frac{dU_p}{dz} \right) \psi_p \right\} = 0. \quad (22)$$

Since

$$(\nabla_T^2 + k_0^2 n_p^2 - \beta_p^2) \psi_p = 0$$

and $n^2 = n_p^2 + \Delta n_p^2$, and dividing with $2i\beta_p$ throughout we get,

$$\sum_p \left(\frac{dU_p}{dz} + i\beta_p U_p + i \left(\frac{k_0^2}{2\beta_p} \right) \Delta n_p^2 U_p \right) \psi_p = 0. \quad (23)$$

Multiplying throughout with ψ_q^* and integrating over the cross section, we get N equations ($q = 1, 2, \dots, N$) relating U_p ,

$$\sum_p \left(M_{qp} \frac{dU_p}{dz} + i\beta_p M_{qp} U_p + i \left(\frac{k_0^2}{2\beta_p} \right) L_{qp} U_p \right) \psi_p = 0, \quad (24)$$

where

$$M_{pq} = \int \psi_p^* \psi_q ds. \quad (25)$$

$$L_{pq} = \int \Delta n^2 \psi_p^* \psi_q ds. \quad (26)$$

These are the general coupled-mode equations. Coupled-mode solutions for specific cases can then be obtained. In the next section, we consider coupled-mode theory for nonparallel waveguides.

3.2. Coupled-mode theory for inclined waveguides

In this section, a method for analysing coupling between inclined waveguides is discussed. The method consists of using different coordinate systems for each of the individual waveguide modes and also the super modes.

The optical waveguide configuration under consideration is shown in Fig. 4. It consists of two planar waveguides A and B separated by d_0 in $z = 0$ plane. The waveguide B is inclined at an angle θ to the waveguide A. The coordinate transformation relations are

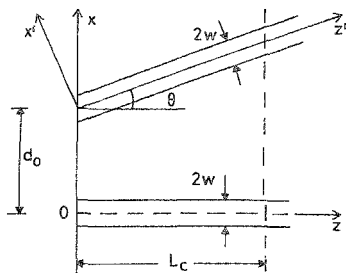


Fig. 4 Schematic of waveguides and coordinate system used in the CMT for inclined waveguides.

$$\begin{aligned} z' &= z \cos \theta + (x - d_0) \sin \theta \\ x' &= -z \sin \theta + (x - d_0) \cos \theta \end{aligned} \quad (27)$$

where d_0 is the waveguide separation at $z = 0$.

The normal mode profiles, the refractive index profiles and the perturbed refractive index profiles of waveguides A and B for the simple planar waveguide coupler are given by

$$n_a^2(x, z) = \begin{cases} n_1^2 & |x| < w \\ n_2^2 & |x| > w \end{cases} \quad (28)$$

$$\Delta n_a^2(x, z) = \begin{cases} n_1^2 - n_2^2 & |x - d_0 - z \tan \theta| < w \sec \theta \\ 0 & \text{otherwise} \end{cases} \quad (29)$$

$$\psi_a^2(x, z) = \begin{cases} C_a \cos(k_f x) & |x| < w \\ C_a \cos(k_f x) e^{-\alpha_c(|x| - w)} & |x| > w \end{cases} \quad (30)$$

Here C_a is the normalization constant. k_f , α_c and C_a can be determined once the numerical values for the structure are specified. Similarly we can write expressions for the other mode in $x'-z'$ plane.

We can consider the interaction to be along z -axis. The instantaneous supermode profile in any z plane $\psi(x, z)$ may be thought of as a combination of uncoupled local normal mode profiles $\psi_a(x, z)$ and $\psi_b(x', z')$ with varying $U_a(z)$ and $U_b(z)$ as below.

$$\psi(x, z) \approx U_a(z) \psi_a(x) e^{-i\beta_a z} + U_b(z) \psi_b(x') e^{-i\beta_b z'} \quad (31)$$

Here, U_a and U_b determine the various characteristics of the mode interaction. These are related through the coupled-mode equations.

For propagation in z - x plane the wave equation is,

$$\frac{\partial^2 \Psi}{\partial x^2} + \frac{\partial^2 \Psi}{\partial z^2} + k_0^2 n^2 \Psi = 0. \quad (32)$$

Substituting eqn (31) in eqn (32), we get,

$$\begin{aligned} & U_a(z) \frac{d^2 \Psi(x)}{dx^2} e^{-i\beta_a z} + U_b(z) \frac{\partial^2}{\partial x^2} \{ \Psi_b(x') e^{-i\beta_b z'} \} \\ & + \Psi_a(x) \frac{\partial^2}{\partial z^2} \{ U_a(z) e^{-i\beta_a z} \} + \frac{\partial^2}{\partial z^2} \{ U_b(z) \Psi_b(x') e^{-i\beta_b z'} \} \\ & + k_0^2 n^2 U_a(z) \Psi_a e^{-i\beta_a z} + k_0^2 n^2 U_b(z) \Psi_b e^{-i\beta_b z'} = 0. \end{aligned} \quad (33)$$

Simplifying this, while noting that individual waveguide modes satisfy corresponding wave equation in their respective coordinate system, we get,

$$\begin{aligned} & k_0^2 \Delta n_a^2 U_a(z) \Psi_a(x) e^{-i\beta_a z} + k_0^2 \Delta n_b^2 U_b(z) \Psi_b(x') e^{-i\beta_b z'} \\ & - 2i\beta_a \frac{dU_a}{dz} e^{-i\beta_a z} \Psi_a + 2 \frac{dU_b}{dz} \frac{\partial}{\partial z} \{ \Psi_b(x') e^{-i\beta_b z'} \} = 0. \end{aligned} \quad (34)$$

Now we require the evaluation of Ψ_b and its derivative in the common coordinate system, *i.e.*, in x - z coordinates. This can be readily done if the field variation in the perturbed region is known. Since planar waveguides have exponentially varying fields in the perturbed region we can proceed as below.

$$\begin{aligned} \frac{\partial}{\partial z} \{ \Psi_b(x') e^{-i\beta_b z'} \} &= \frac{\partial}{\partial z'} \{ \Psi_b(x') e^{-i\beta_b z'} \} \frac{\partial z'}{\partial z} + \frac{\partial}{\partial x'} \{ \Psi_b(x') e^{-i\beta_b z'} \} \frac{\partial x'}{\partial z} \\ &= \Psi_b(x') (-i\beta_b) e^{-i\beta_b z'} \cos \theta + \frac{d\Psi_b}{dx'} e^{-i\beta_b z'} (-\sin \theta). \end{aligned} \quad (35)$$

Equation (34) can now be rewritten as

$$\begin{aligned} & k_0^2 \Delta n_a^2 U_a(z) \Psi_a(x) e^{-i\beta_a z} + k_0^2 \Delta n_b^2 U_b(z) \bar{\Psi}_b e^{-i\beta_b z} \\ & - 2i\beta_a \frac{dU_a}{dz} e^{-i\beta_a z} \Psi_a - 2i\beta_b' \frac{dU_b}{dz} e^{-i\beta_b z} \bar{\Psi}_b = 0. \end{aligned} \quad (36)$$

Now multiplying eqn (36) successively with $\Psi_a^*(x) e^{i\beta_a z}$ and $\Psi_b^*(x) e^{i\beta_b z}$ and integrating with respect to x , we get

$$\begin{aligned} & k_0^2 U_a e^{-(\alpha_a + \alpha_b')} \int \Delta n_{a0}^2 \Psi_a \Psi_a^* dx + k_0^2 U_b e^{i\Delta\beta z} \int \Delta n_b \bar{\Psi}_b \Psi_b^* dx \\ & - 2i\beta_a \frac{dU_a}{dz} \int \Psi_a \Psi_a^* dx - 2i\beta_b' \frac{dU_b}{dz} e^{i\Delta\beta z} \int \bar{\Psi}_b \Psi_b^* dx = 0 \end{aligned} \quad (37)$$

and

$$\begin{aligned}
 & k_0^2 U_a e^{-(\alpha_a + \alpha'_a)z} e^{i \tan \theta z} e^{-i \Delta \beta' z} \int \Delta n_{a0}^2 \Psi_a \Psi_a^* dx + k_0^2 U_b \int \Delta n_b^2 \tilde{\Psi}_b(x) \Psi_b^*(x) dx \\
 & - 2i \beta_a \frac{dU_a}{dz} e^{-i \Delta \beta' z} \int \Psi_a \Psi_b^* dx - 2i \beta_b \frac{dU_b}{dz} \int \tilde{\Psi}_b \Psi_a^* dx = 0
 \end{aligned} \quad (38)$$

where

$$\begin{aligned}
 \alpha_c &= \sqrt{k_0^2 n^2 - \beta_b^2} \\
 \beta'_b &= \beta_b \cos \theta - i \alpha_c \sin \theta \\
 \Delta \beta' &= \beta_a - \beta'_b = \beta_a - \beta_b \cos \theta + i \alpha_c \sin \theta \\
 \Delta \beta'^* &= \beta_a - \beta'_b^* = \beta_a - \beta_b \cos \theta - i \alpha_c \sin \theta \\
 \alpha_c &= \alpha_c \cos \theta + i \beta_b \sin \theta \\
 \alpha_c'^* &= \alpha_c \cos \theta - i \beta_b \sin \theta.
 \end{aligned} \quad (39)$$

For identical planar waveguides the following are the expressions for coupled-mode equations, coupling coefficients, etc.

$$\frac{dU_a}{dz} = i K_{ab} e^{-i \Delta \beta z} e^{-\alpha_c \tan \theta z} U_b \quad (40)$$

$$\frac{dU_b}{dz} = i K_{ba} e^{i \Delta \beta z} e^{-\alpha_c \tan \theta z} U_a \quad (41)$$

and

$$K_{ab} = \frac{k_0^2 \int \Psi_a^* \Delta n_b^2 \Psi_b dx}{2 \beta_a \int \Psi_a^2 dx} \quad (42)$$

$$\begin{aligned}
 K_{ba} &= \frac{k_0^2 \int \Psi_b^* \Delta n_b^2 \Psi_a dx}{2 \beta_b \frac{\sin \theta}{2i \beta_a} \int \frac{\partial \Psi_a^2}{\partial z} dx + \cos \theta \int \Psi_b^2 dx} \\
 &\equiv \frac{k_0^2 \int \Psi_b^* \Delta n_b^2 \Psi_a dx}{2 \beta_a \cos \theta \int \Psi_b^2 dx}.
 \end{aligned} \quad (43)$$

If we consider the step-index planar waveguides, the following coupled-mode solutions can be obtained. From coupled-mode equations we note that the required phase-matching condition is $\beta_a = \beta_b \cos \theta = \beta$, say. The coupling parameters K_{ab} and K_{ba} reduce to those of the coupling coefficient for a directional coupler with the initial gap, *i.e.*, $K = K_{ab} = K_{ba}$. Assuming $U_a = 1$ and $U_b = 0$ at $z = 0$ we can solve eqns (40) and (41) directly resulting in

$$U_a = \cos \left\{ \frac{K}{\alpha_c \tan \theta} \left(1 - e^{-\alpha_c \tan \theta z} \right) \right\}$$

$$U_b = i \sin \left\{ \frac{K}{\alpha, \tan \theta} \left(1 - e^{-z\alpha, \tan \theta} \right) \right\}.$$

The following approximations were made in deriving the coupled-mode equations and the solutions given above.

$$\left| \frac{d^2 U_a}{dz^2} \right| \ll \left| \beta_a \cdot \frac{dU_a}{dz} \right|, \text{ etc.}$$

This implies that U_a varies slowly compared to $\exp(-i\beta_a z)$ along z .

$$\int \Delta n_a^2 \psi_a^2 dx \ll \int \Delta n_a^2 \psi_a^* \psi_b dx.$$

This is valid because in the region of first integration the function varies exponentially whereas in the region of second integration one function is exponential and the other is sinusoidal.

In our case, θ is small so that $\sin \theta \simeq \theta = 0$, $\tan \theta \simeq \theta = 0$ in comparison with $\cos \theta \simeq 1$. But when $\sin \theta$ or $\cos \theta$ is multiplied by z we cannot neglect because z can be large. The approximation is only for the sake of simplifying the final form of equations. The theory of coupled-mode equations derived here is not dependent on this.

In solving the coupled-mode equations, we assumed slow variation of $\exp(-\alpha, \tan \theta z)$, so that the expressions for U_a and U_b are simple.

3.3. Application to Cerenkov SHG

We have extended the coupled-mode theory to analyse the Cerenkov-type SHG. In this case, the SHG wave propagates at an angle to the guided mode. Since the old CMT does not consider the angle of propagation between the interacting modes, the overlap factor between the fundamental and second harmonic modes obtained using old CMT is incorrect. The overlap factor can be improved by incorporating the angle of propagation as in the present case. To do this we make use of the theory discussed in Section 3.2.

The perturbed wave equation is given by⁸,

$$\nabla^2 \psi(x, z, t) - \mu \epsilon \frac{\partial^2}{\partial t^2} \psi(x, z, t) = \mu \frac{\partial^2}{\partial t^2} [P_{NL}(x, z, t)]_y. \quad (44)$$

The total field for the present case can be written as the linear combination of fundamental wave at ω and the second harmonic wave at 2ω , i.e.,

$$\psi(x, z) = U_a(z) \psi_a(x) \exp[i(\omega t - \beta_a z)] + U_b(z) \psi_b(x') \exp[i(2\omega t - \beta_b z')] \quad (45)$$

and the nonlinear polarization is given by

$$[P_{NL}(x, z, t)]_y = dU_a^2(z) \psi_a^2(x) \exp(2\omega t - 2\beta_a z) \quad (46)$$

where, respectively, $U_a(z)$ and $U_b(z)$ are the mode field amplitudes of the fundamental and the second harmonic pump fields, ξ_a and ξ_b , the transverse field distributions of the fundamental and the second harmonic modes, β_a and β_b , the propagation constants of fundamental and second harmonic mode and d is the effective nonlinear coefficient.

Substituting eqns (45) and (46) in eqn (44) and following the same procedure as outlined in Section 3.1 the following equation can be derived,

$$\begin{aligned} & -2i\beta_a \frac{\partial U_a(z)}{\partial z} \psi_a(x) \exp[i(\alpha x - \beta_a z)] + 2 \frac{\partial U_b(z)}{\partial z} \frac{\partial}{\partial z} \{\psi_b(x')\} \exp[i(2\alpha x - \beta_b z')] \\ & = -4\mu_0 \omega^2 d U_a^2 \psi_a^2(x) \exp[i(2\alpha x - 2\beta_a z)]. \end{aligned} \quad (47)$$

Now, the second term on the left-hand side can be written as

$$\begin{aligned} & \frac{\partial}{\partial z} \{\psi_b(x') \exp[i(2\alpha x - \beta_b z')]\} = \\ & \frac{\partial}{\partial z'} \{\psi_b(x') \exp[i(2\alpha x - \beta_b z')]\} \frac{\partial z'}{\partial z} + \frac{\partial}{\partial x'} \{\psi_b(x') \exp[i(2\alpha x - \beta_b z')]\} \frac{\partial x'}{\partial z} \\ & - i\beta_b \psi_b(x') \exp[i(2\alpha x - \beta_b z')] \cos \theta + \frac{\partial \psi_b(x')}{\partial x'} \exp[i(2\alpha x - \beta_b z')] \sin \theta. \end{aligned} \quad (48)$$

Substituting eqn (48) in (47), we get,

$$\begin{aligned} & -2i\beta_a \frac{\partial U_a(z)}{\partial z} \psi_a(x) \exp[i(\alpha x - \beta_a z)] - 2i\beta_b \frac{\partial U_b(z)}{\partial z} \psi_b(x') \exp[i(2\alpha x - \beta_b z')] \cos \theta \\ & - 2 \frac{\partial U_b(z)}{\partial z} \frac{\partial \psi_b(x')}{\partial x'} \exp[i(2\alpha x - \beta_b z')] \sin \theta \\ & = -4\mu_0 \omega^2 d U_a^2 \psi_a^2(x) \exp[i(2\alpha x - 2\beta_a z)] \end{aligned} \quad (49)$$

where θ is the angle at which the second harmonic wave is radiated which is given by $\theta = \cos^{-1} \left(\frac{N_{eff}^\omega}{n_s^{2\omega}} \right)$, N_{eff}^ω , the effective refractive index of the waveguide at the fundamental wavelength, and $n_s^{2\omega}$, the substrate refractive index at the second harmonic wavelength.

The term $\psi_b(x')$ and its derivative in the above equation can be transformed into the common coordinate system, x - z , using eqn (27), by assuming a cosine variation of second harmonic mode in the interaction region, as follows,

$$\begin{aligned} & \psi_b(x') \exp[i(2\alpha x - \beta_b z')] \\ & = E_s \cos[k_s(x \cos \theta - z \sin \theta)] \exp\{i[2\alpha x - \beta_b(x \sin \theta + z \cos \theta)]\} \end{aligned}$$

$$= \frac{E_s}{2} e^{i2\alpha z} \left\{ e^{ik_s^+ x} e^{-i\beta_b^- z} + e^{-ik_s^+ x} e^{-i\beta_b^- z} \right\} \quad (50)$$

and

$$\frac{\partial}{\partial x'} \psi_b(x') \exp[i(2\alpha x' - \beta_b z')] = \frac{E_s}{2} e^{i2\alpha x'} k_s \left\{ e^{ik_s^+ x} e^{-\beta_b^- z} + e^{ik_s^- x} e^{-\beta_b^- z} \right\} \quad (51)$$

where

$$\begin{aligned} k_s' &= k_s \cos \theta - \beta_b \sin \theta \\ k_s'' &= k_s \cos \theta + \beta_b \sin \theta \\ \beta_b' &= \beta_b \cos \theta + k_s \sin \theta \\ \beta_b'' &= \beta_b \cos \theta - k_s \sin \theta \end{aligned} \quad (52)$$

Substituting eqns (50) and (51) in (49) and simplifying, we get,

$$\begin{aligned} & 2i\beta_a \frac{\partial U_a(z)}{\partial z} \psi_a(x) \exp[i(\alpha x - \beta_a z)] \\ & + 2 \frac{dU_b(z)}{dz} \left[i \frac{E_s}{2} e^{i2\alpha x} \left(\beta_b'' e^{ik_s^+ x} e^{-i\beta_b^- z} + \beta_b^- e^{-ik_s^+ x} e^{-i\beta_b^- z} \right) \right] \\ & = 4\mu_o \omega^2 dU_a^2 \psi_a^2(x) \exp[i(2\alpha x - 2\beta_a z)]. \end{aligned} \quad (53)$$

By noting that $k_s \cos \theta = \beta_b \sin \theta$ and denoting

$$\begin{aligned} \frac{1}{2} E_s \exp(ik_s^+ x) &= \psi_b^-(x) \\ \frac{1}{2} E_s \exp(ik_s^- x) &= \psi_b''(x) \end{aligned} \quad (54)$$

we have

$$\begin{aligned} & 2i\beta_a \frac{\partial U_a(z)}{\partial z} \psi_a(x) \exp[i(\alpha x - \beta_a z)] \\ & + 2i \frac{dU_b(z)}{dz} \left[\beta_b'' E_s e^{i(2\alpha x - \beta_b^- z)} + \beta_b^- \psi_b''(x) e^{i(2\alpha x - \beta_b^- z)} \right] \\ & = 4\mu_o \omega^2 dU_a^2 \psi_a^2(x) \exp[i(2\alpha x - 2\beta_a z)]. \end{aligned} \quad (55)$$

Multiplying by $\psi_b^{*+}(x) \exp[-i(2\alpha x - \beta_b'' z)]$ throughout and integrating over the waveguide cross section, we get,

$$\begin{aligned} & 2i \frac{dU_b(z)}{dz} \left[\beta_b'' \int \psi_b \int \psi_b^{*+}(x) dx e^{i(\beta_b'' - \beta_b^-)z} + \beta_b^- \int \psi_b^{*+}(x) \psi_b^-(x) dx \right] \mu \\ & = 4\mu_o \omega^2 dU_a^2 \int \psi_a^2(x) \psi_b^{*+}(x) dx \exp[-i(2\beta_a - \beta_b'' z)] \end{aligned} \quad (56)$$

where we have used the approximation,

$$\int \psi_a(x) \psi_b^{**} dx \ll \int \psi_a^* \psi_b^{**} dx.$$

Equation (56) can be written as

$$\frac{dU_b(z)}{dz} = -i2\mu_o\omega^2 dU_a^2 \Gamma e^{-i\Delta\beta z} \quad (57)$$

where

$$\Gamma = \frac{\int \psi_a^2(x) \psi_b^{**}(x) dx}{\left[\beta_b'' \int \psi_b^* \psi_b^{**}(x) dx + \beta_a'' \int \psi_b^{**}(x) \psi_b^*(x) dx \right]}$$

$$\Delta\beta = \beta_b'' - 2\beta_a'' \quad (58)$$

Power generated at the second harmonic wave is given by

$$P^{2\omega} = \int_0^{\infty} |U_b(t)|^2 dk_s'' \quad (59)$$

thus,

$$P^{2\omega} = 4\mu_o^2\omega^4 d^2 (P^\omega)^2 \Gamma^2 \int_0^{\infty} \frac{4\sin^2 \frac{\Delta\beta l}{2}}{\Delta\beta^2} dk_s'' \quad (60)$$

In the Cerenkov-type phase matching, the energy from the fundamental-guided mode at ω is coupled to the continuum radiation modes at 2ω . Thus the generated second harmonic intensity profile is the super position of these radiation fields. The new phase mismatch factor is, $\Delta\beta = \beta_b'' - 2\beta_a''$.

To calculate the power at the second harmonic radiation mode in the case of Cerenkov configuration, the integral is changed to an easier form as follows:

$$\int_0^{\infty} dk_s'' \rightarrow \int_{-\infty}^{\infty} d\beta \rightarrow \int_{-\infty}^{\infty} d\Delta\beta.$$

From eqn (52), we can derive the expression for dk_s'' and $d\beta_b''$, and is given by

$$dk_s'' = d\beta_b \left(\sin\theta - \frac{\beta_b}{k_z} \cos\theta \right)$$

$$d\beta_b'' = d\beta_b \left(\cos\theta + \frac{\beta_b}{k_x} \sin\theta \right) \quad (61)$$

$$d\beta_b'' = -d\Delta\beta.$$

Thus,

$$dk_s'' = d\Delta\beta \frac{\left(\frac{\beta_b}{k_x} \cos\theta - \sin\theta \right)}{\left(\cos\theta + \frac{\beta_b}{k_x} \sin\theta \right)} \quad (62)$$

Solving eqn(59), we get,

$$P^{2\omega} = 16\mu_0^2\omega^4 d^2 (P^\omega)^3 \Gamma^2 2/\pi \frac{(\beta_{k_1}^h \cos\theta - \sin\theta)}{(\cos\theta + \beta_{k_1}^h \sin\theta)} \quad (63)$$

For the limiting case of $\theta=0$, the above equation reduces to the result obtainable using the old scalar coupled-mode theory. Figure 5 shows the plot of variation of SHG efficiency as a function of waveguide thickness. Solid line corresponds to the curve using old scalar CMT, dashed curve to the improved CMT (present case) and dotted line to the method given in Hashimuze *et al*⁹. It may be noted that the inclusion of angle factor in the present theory gives rise to a lower efficiency than predicted by the old CMT as expected. Also due to the fact that at larger waveguide thickness, the angle between the interacting modes is small, the predicted SHG efficiencies by all the three methods are nearly the same. One can thus arrive at certain conclusions regarding the range of applicability of the various theories. The present theory has also been used in the study of SHG in crystal cored fibers¹⁰.

4. Conclusions

Two main methods of analysis are addressed in this review, *viz.*, BPM and CMT. These methods are suitably modified and improved so that light propagation through fiber and integrated optic waveguide structures can be evaluated more correctly. Numerical simulations have been done for some guided wave structures and some results are presented. Wherever possible the present results are compared with other known methods reported in literature so that the usefulness or otherwise of the present theory can be properly assessed.

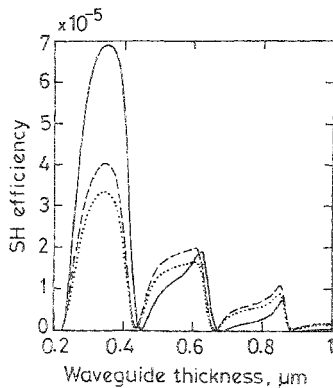


FIG. 5. Comparison of the efficiency of second harmonic generation (SHG) between the present method and the methods reported earlier.

Acknowledgement

The authors wish to express their sincere thanks to T. Srinivas, Shiva Kumar, M.V. Sathyanarayana and R. Mahendra Prabhu for their contributions.

References

- 1 FEIT, M D AND FLECK, J A JR Light propagation in graded index optical fibers, *Appl Opt.*, 1978, **17**, 3990-3998
- 2 VAN ROEY, J., VAN DER DONK, J. AND LAGASSE, P E. Beam propagation method: analysis and assessment, *J Opt. Soc Am.*, 1981, **71**, 803-810
- 3 SHIVA KUMAR, SRINIVAS, T. AND SELVARAJAN, A. Beam propagation method and its application to integrated optic structures and optical fibers, *Pramana*, 1990 **34**, 347-358
- 4 SHIVA KUMAR, SRINIVAS, T. AND SELVARAJAN, A. Transform technique for planar optical waveguides, *J Opt Soc Am A*, 1991, **8**, 1681-1687
- 5 MAHENDRA PRABHU, R. AND SELVARAJAN, A. Analysis of the evanescent field coupling between a fiber and a planar waveguide using the explicit finite difference method with a nonuniform mesh, *Opt Engng.* 1993, **32**, 717-724
- 6 SATHYANARAYANA, M. V., SRINIVAS, T AND SELVARAJAN, A. Electrostatic field analysis in electrooptic devices, *J Electromagnetic Waves Applic.* 1992, **6**, 143-155.
- 7 HAUS, H A AND HUANG, W. Coupled mode theory, *Proc IEEE*, 1991, **79**, 1505-1518
- 8 YARIV, A. Coupled mode theory for guided wave optics, *IEEE J.* 1973, **QE-9**, 919-933
- 9 HASHIZUME, N., KONDO, T., ONDA, T., OGASAWARA, N., UMEGAKI, S AND ITO, R. Theoretical analysis of Cerenkov-type optical second harmonic generation in slab waveguides, *IEEE J.* 1992, **QE-28**, 1798-1815
- 10 BALASUBRAMANIAN, R AND SELVARAJAN, A. Coupled mode analysis of three wave mixing process in crystal cored fibers, *Int J Optoelectron.* 1993, **8**, 385-398